

Evidence for $[2p(s)4f]$ multielectron resonances in x-ray-absorption spectra of sixth-period elements

Andrea Di Cicco

*Dipartimento di Matematica e Fisica, Università degli Studi di Camerino,
Via Madonna delle Carceri, 62032 Camerino (MC), Italy*

Adriano Filipponi

*Dipartimento di Fisica, Università degli Studi dell' Aquila,
Via Vetoio, 67010 Coppito, L'Aquila, Italy*

(Received 1 July 1993; revised manuscript received 19 November 1993)

Clear evidence for multielectron excitation channels involving $2p$ or $2s$ and $4f$ electrons has been discovered in x-ray-absorption L -edge spectra of several sixth-period elements. Measurements on liquid Pb and Bi, as well as in PbO, Pb(CH₃CO₂)₂, and Bi₂O₃ compounds, are reported and compared with previous data on vapor Hg. Onset energies of the double-electron excitation channels are found to be in agreement with previously published self-consistent calculations. A weaker feature, which has been observed in several spectra, is assigned to a triple-electron excitation involving two strongly correlated $4f$ electrons. The importance of these findings for the extended x-ray-absorption fine structure structural analysis of sixth-period elements is discussed.

I. INTRODUCTION

In recent times a careful analysis of x-ray-absorption spectra of several atomic and molecular systems has revealed the presence of a detectable signal from multielectron excitation channels. The general relevance of these phenomena for the understanding of fundamental aspects of atomic physics has been widely discussed in previous papers dealing with noble gases (Ref. 1 and references therein) and third-period elements.² Moreover, multielectron excitation features appear to affect seriously the structural analysis of the x-ray-absorption fine structure (XAFS), thus involving also important practical implications. In fact, it was early recognized that the onsets of double-electron excitation channels, associated with the additional excitation of a shallow core electron, were able to produce steplike atomic backgrounds which could not be accounted for by smooth background models. The occurrence of double-electron excitations in condensed systems was first observed in Si K -edge spectra, where a simultaneous excitation of $1s$ and $2p$ electrons gives rise to the KL -edge feature.³ The presence of these excitations was later found to be a common characteristic of third-period atoms.^{2,4} Direct evidence for the presence of KL shakeup channels in solid systems has been recently obtained, revealing the corresponding photoelectron peaks in x-ray-photoemission spectra (XPS) of Na ionic compounds (in particular NaCl)⁵ and Mg compounds (MgO and MgF₂).⁶ Other examples of the interplay between the XAFS structural oscillations and the multielectron excitation background have been studied in Br compounds,^{7,8} related to the $KM_{2,3}$, $KM_{4,5}$, and KN_1 excitation edges, previously well studied only in the case of Kr.⁹ Other authors proposed a method to iden-

tify the atomic background in condensed systems based on the suppression, by means of an iterative procedure, of the structural signals.¹⁰ They revealed the presence of the $KM_{4,5}$ edge at the Br and Rb edges of RbBr and of another feature after the Pb L_3 edge in PbO₂. The latter was assigned to $4f$ electron shakeup excitations on the basis of the $Z + 1$ approximation. More recently, a study of Hg vapor at the L_3 , L_2 , and L_1 edges provided an unambiguous identification of the onset of shakeup channels associated with $[2p4f]$ and $[2s4f]$ double-hole configurations, which appear to contribute with distinct slope changes in the absorption background, and possibly with $[2p4f^2]$ and $[2s4f^2]$ triple-hole configurations.¹¹

In spite of the large number of investigations in this field, very little attention has been paid to the influence of multielectron excitation features on conventional structural data analysis based on the effective one-electron theory. Early works by Stern and co-workers¹² concentrated mainly on the influence of many-body effects on the intensity of the structural signal (effective amplitude correction S_0^2). In the previously cited works, however, it has been clearly demonstrated^{1-4,7-11} that another important direct many-body effect exists. This is the presence of steplike edges in the atomic cross section, in the XAFS region, associated with the simultaneous excitation, in addition to the main core electron, of shallower core electrons with typical binding energies in the range 20–500 eV.

The present investigation is focused on the atomic background effects associated with the contemporary excitation of a $2p$ (or $2s$) and a $4f$ electron, indicated as $[2p(s)4f]$, occurring above the L edges of sixth-period elements. In particular we shall consider the $4f$ metals Hg, Pb, and Bi, for which low-noise experimental data

have been collected. Previous studies^{10,11} suggested that the occurrence of these phenomena, in sixth-period elements, was rather general. Investigations on the atomic backgrounds are very important in light of various applications of XAFS spectra for structural analysis. For example, an accurate XAFS investigation on the premelting of Hg impurities in Pb (Ref. 13) was performed using the Hg vapor spectrum as atomic background model, a correct procedure whose effectiveness was recognized even before the discovery of the $[2p4f]$ threshold.¹¹ Moreover, structural XAFS investigations at Bi (and sometimes Pb) L edges¹⁴ became quite important in recent times for the discovery of bismuth-based perovskite superconductors. Generally speaking, the effects of multielectron excitation channels presented in this work should be taken into account in any XAFS structural study of L edges of sixth-period elements, including those present in compounds having large technological applications (for example in catalysis) such as Ta, W, Re, Os, Ir, Pt, and Au.

The theoretical predictions of the energy onset of the $[2p(s)4f]$ channels¹¹ indicate a monotonic increase with the atomic number Z . In the lighter sixth-period elements (up to Pt), the onsets lie in a range of about 50–100 eV above the corresponding L edge. However, for the $4f$ metals under consideration, the double-electron excitation threshold is located in the range 100–200 eV. This energy region simplifies the identification of the threshold because the structural signal has a smaller intensity. In any case the presence of the structural signal hinders the certain assignment of the double-electron features, so that the reduction of its intensity is an essential problem to solve. This topic is discussed in Sec. II, where a brief description of the experimental details is also reported. In Sec. III the experimental results for Hg, Pb, and Bi are presented, while in Sec. IV observed results and trends, as well as the implications for applications to structural analysis at these edges, are discussed.

II. EXPERIMENTAL DETAILS

In the case of sixth-period elements, with the exception of Hg, the possibility of measuring x-ray-absorption spectra of isolated atoms is hampered by the small vapor pressures of the elements. Therefore, we selected a certain number of compounds that, in appropriate experimental conditions, are characterized by a small or rapidly decaying structural signal. We identified two different experimental strategies. The first strategy is based on the observation that it is generally possible to select compounds in which the heavy metal binds loosely to low- Z elements, typically organic matter. In this way, since the structural signal associated with O and C atoms is generally confined in the low-energy region, the higher-energy part of the spectra should be affected only by rather smooth oscillations. The second strategy consists in reducing the intensity of the structural signal by taking advantage of the thermally induced damping of the oscillations at high energy. This effect, usually referred to as the Debye-Waller effect,¹⁵ assumes that large-amplitude atomic motion will wash out most of the XAFS oscilla-

tion in the limit of high temperatures, particularly above the melting point of the substances. For this reason we have performed measurements of thin metal foils of pure Pb and Bi, heating the specimen to high temperatures above the respective melting points.

X-ray-absorption measurements near the Bi and Pb L_3 , L_2 , and L_1 edges have been performed in transmission mode at LURE (Laboratoire pour l'Utilisation du Rayonnement Electromagnetique) on the D-42 and D-44 beam lines during dedicated beam time. Pure metals foils of Bi and Pb were measured in the liquid phase at temperatures of 300 °C (Bi) and 350 °C (Pb). A flux of N_2 was maintained inside the furnace to provide an inert atmosphere. Details on the preparation on liquid metal samples, useful to perform structural studies of liquids, will be described elsewhere.¹⁶

Samples of Bi_2O_3 , PbO, and $Pb(CH_3CO_2)_2$ (acetate) powders have been measured at room temperature. In order to produce samples of an appropriate thickness for absorption studies these Bi and Pb compounds were finely ground in a mortar. The powder was dispersed in a nonsolvent liquid and the suspension was allowed to settle for some time to produce a grain-size separation by gravity. The largest particles were excluded by precipitation and the suspension was then filtered through a Millipore polycarbonate membrane. By this procedure, a rather uniform layer of powder was obtained. The polycarbonate substrate material absorbed a negligible amount of x-ray radiation over the energy range under investigation. Bi_2O_3 finely dispersed into a boron nitride matrix was also measured at high temperatures (700 °C).

Sample thickness was always chosen in order to obtain the best signal-to-noise ratio in absorption measurements ($\Delta\mu x \approx 1$ for L_3 edges). Optimization of samples was done in advance by using the XAFS laboratory equipment of the University of Camerino (Centro Interdipartimentale Grandi Apparecchiature).

III. PRESENT EVIDENCE OF MULTIELECTRON RESONANCES

Experimental evidence for shakeup and/or shakeoff of f electrons at the L_3 , L_2 , and L_1 edges of sixth-period atoms will be presented in order of increasing atomic number Z . In particular, in Sec. III A we shall briefly recall the case of Hg vapor, reported in a separate publication.¹¹ In Secs. III B and III C the present measurements on Pb and Bi will be reported, respectively. Results are presented for the pure elements in the liquid phase as well as for the oxides and acetate compounds.

The low-noise XAFS measurements on liquid Bi and Pb have been recorded in the framework of a research project on the study of three-body correlations in liquid metals. In the present paper we focus on the double-electron excitation effects, clearly visible in these spectra. These features are present and detectable also in the spectra of the solid phase but their identification becomes certain only after verifying that they are not affected by thermal damping effects.

Double-electron $[2p(s)4f]$ core-hole resonances contribute with a signal which can amount to a few percent of the main one-electron $L_{2,3}$ or L_1 edges, but nevertheless they are often immediately visible after a careful inspection of the raw data. In order to highlight the double-electron contribution with respect to the structural oscillations, in the following sections x-ray-absorption data will be presented after subtracting an average linear decay and normalizing the spectra to the actual height of the discontinuity of the L edges under consideration. The use of a linear function for absorptance decay after the L edges, evaluated in an extended energy region after the thresholds (specified below), ensures a coherent extraction and an unbiased presentation of features and slope changes associated with double-electron resonances in raw data. Amplitudes of these difference signals, hereafter indicated with $\Delta\alpha$, can be directly compared for each element or compound under investigation. A comparison of the energy onset of double-electron excitation channels in different elements or compounds can be made by considering the "excess energy" required to promote the $4f$ electron to the first available excited state. Therefore spectra are presented by taking as zero energy the inflection point of the L edge under examination, which measures the energy of the first available continuum states for the $2p(s)$ photoelectron with an uncertainty of a few eV. In the following, this energy scale will be denoted by E_t .

A. $Z = 80$ Hg

Direct evidence for the presence of $[2p(s)4f]$ double core-hole resonances in Hg has been obtained in a previous study on Hg vapor.¹¹ In that case, due to the high vapor pressure of Hg, direct absorption measurements on isolated atoms could be performed. An evident slope change, occurring about 135 eV beyond the L edges, was unambiguously identified and assigned to the onset of the $[2p(s)4f]$ double-excitation channels on the basis of Dirac-Fock self-consistent-field (SCF) calculations. Very similar spectra were obtained for the L_3 and L_2 edges [slope changes were $2.0(2) \times 10^{-4} \text{ eV}^{-1}$ for both cases], while the L_1 edge was characterized by a large hump near the energy threshold. Taking account of these anomalies turned out to be extremely important in extracting the structural signal in condensed phases of Hg, and especially in the liquid phase where its intensity appears to be strongly damped.¹⁷

Besides the strong $[2p(s)4f]$ feature, the Hg vapor spectra show an additional smoother slope change around 300 eV above the edge. A tentative assignment involving triple-electron excitations, supported by SCF Dirac-Fock calculations, was proposed.¹¹

B. $Z = 82$ Pb

In Fig. 1 the Pb L_3 and L_1 normalized absorption $\Delta\alpha(E_t)$ of liquid Pb at a temperature of 350 °C and Pb acetate at room temperature are shown. The L_3 spec-

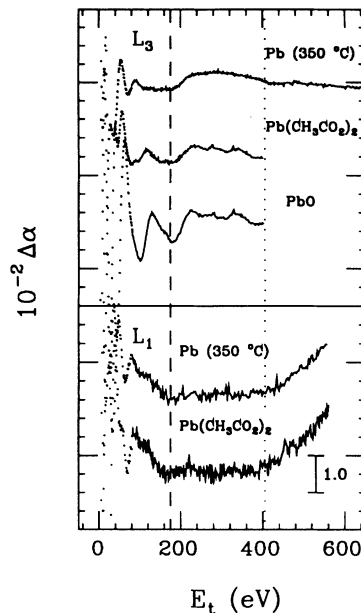


FIG. 1. Experimental deviations $\Delta\alpha$ from the average linear decay as a function of E_t for liquid lead ($T = 350^\circ\text{C}$) and $\text{Pb}(\text{CH}_3\text{CO}_2)_2$ at the L_3 (upper panel) and L_1 edges (lower panel), and for PbO at the L_3 edge (upper panel). The $[2p(s)4f]$ onset energy is indicated by a vertical dashed line, while a further feature (a slope change), appearing at the correct excess energy associated with a $[2p(s)4f^2]$ excitation, is indicated by the dotted line.

trum of PbO , which shows a stronger structural signal than lead acetate, is also reported. In these cases the average linear decay has been interpolated in the range $E_t \in [50, 950] \text{ eV}$ and $E_t \in [30, 560] \text{ eV}$ for L_3 and L_1 spectra respectively.

The L_3 experimental deviations $\Delta\alpha(E_t)$ reported in Fig. 1 (upper panel) show unambiguously the presence of a steplike edge occurring at about 180 eV above the inflection points. The energy onset is in perfect agreement with the previous predictions ($\approx 175 \text{ eV}$) for the excess energy necessary to excite a $4f$ electron simultaneously with the $2p$ one, in the Pb atom.¹¹ The smooth opening of this channel, which rises up to about 50 eV beyond 180 eV, can be easily identified in raw data and is a common characteristic of the L_3 spectra. It is interesting to note that the overall shape of the double-electron excitation channel is very similar for liquid Pb, Pb acetate, and PbO , if we consider the presence in the latter two spectra of some residual structural signal above 200 eV. In particular, the height and the edge onset shape are very similar in all spectra of Fig. 1. The discontinuity due to the $[2p4f]$ channel can be estimated to be about 0.5% of the main $[2p]$ channel. Previous measurements¹⁸ on liquid Pb could not detect such multielectron features because they were limited to an energy region of about 200 eV above the L_3 edges.

The L_1 spectra show a different behavior: they present a clear slope change of about $1.2 \times 10^{-4} \text{ eV}^{-1}$ at the same excess energy ($\approx 180 \text{ eV}$) as found in the L_3 cases (slightly lower for Pb acetate). Of course, the possible presence of

a steplike shape for the $[2s4f]$ channel (of small intensity and with a very smooth onset) is not ruled out, but our empirical method of subtraction reveals in this case only the slope change. However, differences between $[2p4f]$ and $[2s4f]$ double-electron excitation channels in Pb are not surprising since the dipole-allowed interacting final states can generate different features in the cross sections.

Both in the L_1 and in L_3 (only liquid Pb at 350 °C) spectra a second slope change is easily identified at an energy of about 400 eV. In the L_1 spectra the slope change amounts to about $0.9 \times 10^{-4} \text{ eV}^{-1}$, while in the L_3 case it is about $0.3 \times 10^{-4} \text{ eV}^{-1}$. This second feature is located at the excess energy associated with a triple-electron excitation $[2p(s)4f^2]$ and will be discussed with more detail in Sec. IV.

C. $Z = 83$ Bi

Bismuth is one of the heaviest elements that can be investigated in macroscopic quantities and certainly the last of the sixth-period that can be prepared in suitable form for x-ray-absorption studies. As far as the onset of the $[2p(s)4f]$ double-electron excitation is concerned, theory predicts an excess energy of about 195 eV with respect to the L -edge thresholds.¹¹

Two Bi compounds have been investigated in the present context: the first is a Bi metal foil measured at high temperature in the liquid phase as described in Sec. II, and the second is Bi_2O_3 . The difference spectra $\Delta\alpha(E_t)$ for the three L edges of Bi metal are shown in Fig. 2. An evident feature is observed at about 200 eV after each of the three L edges (vertical dashed line). This

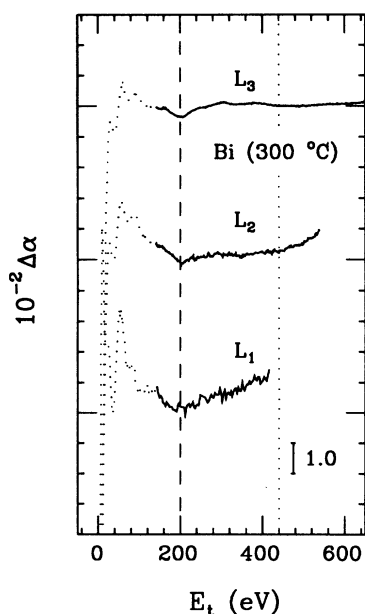


FIG. 2. Experimental deviations $\Delta\alpha$ from the average linear decay as a function of E_t for liquid bismuth ($T = 300^\circ\text{C}$) for the L_3 , L_2 , and L_1 edges. Experimental onsets of the many-electron channels $[2p(s)4f]$ and $[2p(s)4f^2]$ are indicated by dashed and dotted lines, respectively.

anomaly of the atomic background is associated with the onset of the $[2p(s)4f]$ double-electron excitation channels. In the L_3 and L_2 cases both a steplike shape and a slope change can be identified for the $[2p4f]$ channel. The slope changes calculated in the first 100 eV above the edges, which can be determined with good accuracy, amount to about $1.4 \times 10^{-4} \text{ eV}^{-1}$ in both cases. The L_1 spectrum of liquid Bi shows a similar slope change amounting to about $1.5 \times 10^{-4} \text{ eV}^{-1}$ associated with the $[2s4f]$ channel. The slope discontinuities are of the same order as those found in the Hg case. As a further confirmation of the atomic nature of the slope change, one can observe that, while the structural oscillations are different between L_3 or L_2 spectra and the L_1 spectrum, the double-excitation features are instead very similar in all edges. The detection of these clear slope discontinuities in liquid bismuth, where structural oscillations are almost damped beyond 200 eV, suggests that taking account of this feature is necessary in any accurate structural data analysis at the Bi L edges.

Also in liquid Bi a broader slope change, which can be associated with a triple-electron excitation, is detected in the L_2 and L_3 spectra around 440 eV. The possible assignment for this feature will be discussed in more detail in the next section.

Bi_2O_3 is the most common oxide of bismuth. As far as the double-electron excitation is concerned, this compound presents the advantage of having Bi bonded to a very light atom, O, with a scattering power confined to low photoelectron energies. Besides, due to the low-symmetry crystalline structure of $\alpha\text{-Bi}_2\text{O}_3$ there are several different distances in the nearest coordination shells [Bi-O and Bi-(O)-Bi]. In particular, there is a wide distribution of Bi-O distances in the range 2.13–2.8 Å.

Room-temperature x-ray-absorption measurements of $\alpha\text{-Bi}_2\text{O}_3$ have been performed and the results for the Bi L_3 and L_1 edges are reported in Fig. 3. In the same figure (center curve) we also report the L_3 spectrum measured at 700 °C. The contribution of the $[2p4f]$ channel to the atomic background (onset energy indicated by the vertical dashed line), although clearly visible in the room-temperature spectrum (upper curve), is better evidenced in the high-temperature one, where the structural signal is almost suppressed. There is also evidence of the $[2s4f]$ channel in the L_1 spectrum (lower curve). From the spectra of Fig. 3 it is possible to evaluate the intensity of the $[2p(s)4f]$ channels. They appear to have a steplike shape with a smooth onset and a step discontinuity of about 0.5% of the main one-electron channel. Differences between atomic background shapes in Bi_2O_3 and liquid Bi are not surprising since the final-state electron orbitals involved in the excitation process are completely different in the two cases and are generally affected by the chemical environment.

Room-temperature spectra reported in Fig. 3 are a good example of how atomic double-electron features and structural signals interfere. A coarse data analysis performed by using a smooth monotonic atomic background and Fourier filtering would not reveal the presence of the double excitation at about 200 eV, yielding a distorted structural contribution. As an example, the min-

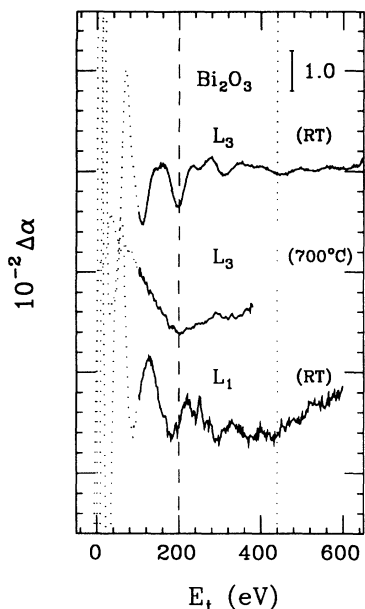


FIG. 3. Experimental deviations $\Delta\alpha$ from the average linear decay as a function of E_t for Bi_2O_3 for the L_3 and L_1 edges. Vertical dashed and dotted lines have the same meaning as in Fig. 2.

ima around 200 eV in Bi_2O_3 at all the edges are clearly enhanced by the background features. Structural parameters determined by XAFS, and particularly those related to the amplitude of the signals, would be affected by a systematic error due to the existence of multielectron features in the atomic background.

Finally, it is interesting to note that even in this compound a further weak anomaly, indicated by the vertical dotted line, is clearly seen in the experimental $\Delta\alpha$ room-temperature spectra around $E_t = 440$ eV. This feature appears as a slope change and is naturally related to the one observed in liquid Bi. Its interpretation will be discussed in the next section.

IV. DISCUSSION

As reported in previous sections, the double-electron excitation features associated with the $[2p(s)4f]$ configuration have been observed in a large number of compounds of several sixth-period elements. They can no longer be regarded as peculiar features present in the spectra of gas-phase closed-shell atoms (like Hg) or in particular condensed aggregates of matter. Instead they appear to be a general characteristic of L -edge spectra of any sixth-period element having a filled $4f$ shell. This latter requirement ensures that the $4f$ level does not participate in valence bonding, and its binding energy exceeds a magnitude of a few eV. The presence of these features appears to be independent of the compound under investigation, while their shape sometimes appears to be dependent on the particular compound and edge under consideration. All of these findings can be interpreted within the general scheme where the major effects

are driven by atomic properties, such as the presence and the energy of the $4f$ level, while many minor details are instead dependent on the actual excited-electron final-state wave functions, which are strongly influenced by the chemistry of the compound.

Let us briefly summarize the present experimental evidence. Mercury has been carefully studied in the gas phase¹¹ providing unambiguous evidence for the $[2p(s)4f]$ resonances. These features have also been detected in liquid phase studies with similar characteristics.¹⁷ Lead was actually the first element where these features were isolated,¹⁰ and in this paper we present further extensive evidence at the L_3 and L_1 edges of liquid Pb, at the L_3 and L_1 edges of lead acetate, and at the L_3 edge of PbO . Finally, liquid bismuth has shown the presence of $[2p(s)4f]$ resonances at the L_3 , L_2 , and L_1 edges, while related features have also been observed in Bi_2O_3 .

The spectral shape of the multielectron excitation anomalies in sixth-period elements can be usually regarded as a slope change while sometimes a clear steplike shape is detected. Calculated shakeoff cross sections in the Kr case show a monotonic increase as a function of energy.¹ In sixth-period atoms a similar qualitative behavior of intense shakeoff channels can result in the observed slope changes. On the other hand, shakeup transitions to discrete states are likely to result in steplike shapes of the partial cross section, as also shown in krypton, where single shakeup intensities saturate early as a function of energy. On the basis of these results, one can speculate that shakeoff processes dominate when only a slope change is observed and that transitions to quasidecrete states are revealed by the detection of the steplike edges. However, the observed shapes of the multielectron channels are difficult to model accurately because of the number of possible final-state configurations and the difficulties in taking proper account of the interactions. For these reasons, the actual shape of the $[2p(s)4f]$ channel can depend on the atomic number, on the L edge under consideration, and on the chemistry of the compound. Certainly, further experimental evidence in other sixth-period atoms will help in clarifying the trends in the shape of the multielectron excitation channels.

In Table I we summarize the presently available results for sixth-period atoms by listing, for each element and L -edge type, the compounds being examined and the major features that cannot be attributed to any structural origin. Experimental onset energies E_t and shapes and intensities associated with the $[2p(s)4f]$ double-electron channels are all reported in Table I. The onset energies correspond to the observed slope changes in the experimental spectra and are evaluated by intersecting two best-fit straight lines calculated in a region of 50–100 eV before and after the threshold of the many-electron channels. Error bars reported in Table I (in parentheses) include the dispersion of the intersection points as well as possible errors in defining the E_t energy scale. Onset energy values have been rounded according to the magnitude of the error bar.

Only in Pb L_3 and Bi_2O_3 L_3 and L_1 spectra has a clear steplike shape been recognized. In the PbO_2 case

the atomic background extracted by means of a different procedure has shown a steplike shape as well.¹⁰ The energy value for the onset is reported for comparison in Table I. It should be noted that the apparent disagreement probably reflects the difficulties in defining E_t correctly and the differences in the analysis procedures. In addition to this main feature, which appears at E_t approximately equal to 135 eV in Hg, 180 eV in Pb, and 200 eV in Bi, another slope change has been very often identified in the high-energy side of the spectra. This slope change appears to be characterized by a smoother onset than the $[2p(s)4f]$ features and for this reason the spectral shape is less accurate. However, its existence is supported by a wide range of evidence. It appears to occur systematically at an energy slightly higher than twice the E_t associated with the $[2p(s)4f]$ feature. This occurrence suggests that it is associated with the onset of triple-electron excitations involving one $2p$ (or $2s$) and two $4f$ electrons. Usually, triple-electron excitations are considered to have such a tiny intensity as to prevent experimental detection. In this case, the relatively intense features could be due to the strong correlation between the $4f$ electrons in these heavy ions. The identification of this multielectron channel was suggested previously in the case of Hg vapor measurements¹¹ on the basis of self-consistent energy calculations predicting an additional energy of about 298 eV, and this hypothesis can now be tested on a wider experimental basis. The position and intensity of the feature assigned to the $[2p(s)4f^2]$ channel is indicated in the last three columns of Table I. The energy positions of this feature in the Pb and Bi cases are consistent with the expected energy required to extract two $4f$ electrons.

An interesting detail of the double-electron features, supporting the experimental identifications in comparison with the theoretical prediction, is the observation of trends as a function of the atomic number. The onset of the $[2p(s)4f]$ channels occurs at successively higher energies as a function of Z , as already shown in the previous

sections. In a previous paper¹¹ a diagram reporting the theoretical onset energies from $Z = 72$ to $Z = 86$ was reported. The monotonic increase predicted by theory can now be verified experimentally. The comparison of the values reported in Table I with the theoretical onset estimates¹¹ can be visualized in a comprehensive plot. The $L_3 \Delta\alpha$ difference spectra for Hg vapor and liquid Pb and Bi are shown on the same E_t energy scale in Fig. 4, where the increasing onset energy trend with increasing Z is evident. The observed energy onsets of the $[2p(s)4f]$ double-electron channels compare nicely with theoretical estimates for the $4f \rightarrow 5f$ shakeup channels calculated in the δ_{DF} approximation (self-consistent Dirac-Fock relativistic wave functions were used). The comparison of experimental data with available δ_{DF} calculations and with less accurate estimates given by the $Z + 1$ approximation is given in Fig. 5. The agreement with self-consistent calculation is excellent.

As a final remark we would like to address the problem of the relevance of these findings to structural studies at the L edges of sixth-period elements. Previous XAFS studies limited to photoelectron wave vectors larger than $k = 4 \text{ \AA}^{-1}$ were affected by the $[2p(s)4f]$ features starting with W ($Z = 74$). Heavier elements presented this feature at systematically higher k values up to about $k = 7 \text{ \AA}^{-1}$ in Bi ($Z = 83$). This feature is therefore affecting the relatively low-energy part of the XAFS oscillation, if it is considered that typical spectra have an extension of even 1000 eV ($k \approx 15 \text{ \AA}^{-1}$) at these edges. Nevertheless, it is quite surprising that nobody ever realized their presence when attempting structural analysis. A possible explanation can be found in the relatively weak intensity and low frequency (in k space) of these features, which have contributed to hide them in the usual Fourier transform analysis. It is only when experimental signals are compared with accurate one-electron theoretical calculations that the anomalies associated with multielectron features are clearly evidenced.^{4,7,8} The importance of taking account of the many-electron excitations for ob-

TABLE I. Experimental onset energies E_t and intensities of the $[2p(s)4f]$ and $[2p(s)4f^2]$ multi-electron excitation resonances. Sl indicates a slope change, and St a steplike shape.

Element	Edge	Compound	$[2p(s)4f]$			$[2p(s)4f^2]$		
			E_t (eV)	Type	Intensity	E_t (eV)	Type	Intensity
Hg	L_3	Hg vapor ^a	135(5)	Sl	$2.0(2) \times 10^{-4} \text{ eV}^{-1}$			
Hg	L_2	Hg vapor ^a	135(5)	Sl	$2.0(2) \times 10^{-4} \text{ eV}^{-1}$			
Hg	L_1	Hg vapor ^a	125(5)					
Pb	L_3	liquid Pb	180(10)	St	$0.5(1) \times 10^{-2}$	410(10)	Sl	$0.3(1) \times 10^{-4} \text{ eV}^{-1}$
Pb	L_1	liquid Pb	180(10)	Sl	$1.2(2) \times 10^{-4} \text{ eV}^{-1}$	410(10)	Sl	$0.9(2) \times 10^{-4} \text{ eV}^{-1}$
Pb	L_3	PbO	180(20)	St	$0.5(2) \times 10^{-2}$			
Pb	L_3	PbO ₂ ^b	163(5)	St				
Pb	L_3	Pb(CH ₃ CO ₂) ₂	180(10)	St	$0.5(1) \times 10^{-2}$			
Pb	L_1	Pb(CH ₃ CO ₂) ₂	170(10)	Sl	$1.2(1) \times 10^{-4} \text{ eV}^{-1}$	400(10)	Sl	$0.9(2) \times 10^{-4} \text{ eV}^{-1}$
Bi	L_3	liquid Bi	200(10)	Sl	$1.4(2) \times 10^{-4} \text{ eV}^{-1}$	440(10)	Sl	$0.3(1) \times 10^{-4} \text{ eV}^{-1}$
Bi	L_2	liquid Bi	200(10)	Sl	$1.4(2) \times 10^{-4} \text{ eV}^{-1}$	440(10)	Sl	$0.4(2) \times 10^{-4} \text{ eV}^{-1}$
Bi	L_1	liquid Bi	200(10)	Sl	$1.5(2) \times 10^{-4} \text{ eV}^{-1}$			
Bi	L_3	Bi ₂ O ₃	200(10)	St	$0.5(1) \times 10^{-2}$	440(10)	Sl	$0.3(1) \times 10^{-4} \text{ eV}^{-1}$
Bi	L_1	Bi ₂ O ₃	200(20)	St	$0.5(2) \times 10^{-2}$	440(10)	Sl	$0.9(2) \times 10^{-4} \text{ eV}^{-1}$

^aReference 11.

^bReference 10.

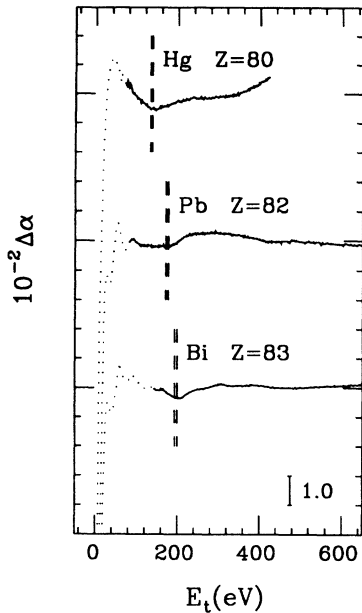


FIG. 4. Comparison of the $\Delta\alpha$ signals for increasing atomic number: L_3 edges of atomic Hg, liquid Pb ($T = 350^\circ\text{C}$), and liquid Bi ($T = 300^\circ\text{C}$). Theoretical predictions, based on relativistic self-consistent calculations of onset energies of the $[2p4f]$ two-electron excitation channel, are indicated by vertical dashed lines.

taining accurate structural parameters in XAFS analysis can now be easily recognized.

V. CONCLUSIONS

We presented low-noise x-ray-absorption measurements at the Pb and Bi L edges in liquid bismuth, liquid lead, their oxides, and lead acetate, showing clear evidence of anomalies of the underlying atomic background due to multielectron excitations involving $4f$ electrons. The same features were previously identified only in Hg vapor (Ref. 11) and PbO_2 .¹⁰

The energy onsets of the $[2p(s)4f]$ double-electron excitations agree quite well with relativistic self-consistent calculations (about 175 eV excess energy in Pb and 195 eV in Bi). Double-electron channels have been classified according to the observed shape, a slope discontinuity and/or a steplike edge. The intensity of the double-electron contribution has been estimated by measuring the slope change or the step height. Slope changes are found of the order of 10^{-4} eV^{-1} and step heights of the order of 0.5% of the main L discontinuity (Pb case). Evidence of a further feature at higher energies (about 400 eV excess energy in Pb and 440 eV in Bi), which appears as a smoother slope change, has been found whenever data have been collected at those energies. These additional features are located at the correct excess energies associated with a simultaneous excitation of three electrons $[2p(s)4f^2]$. Intensities of the slope changes are weaker but clearly detectable. The relatively large contribution due to this triple-excitation channel could be due

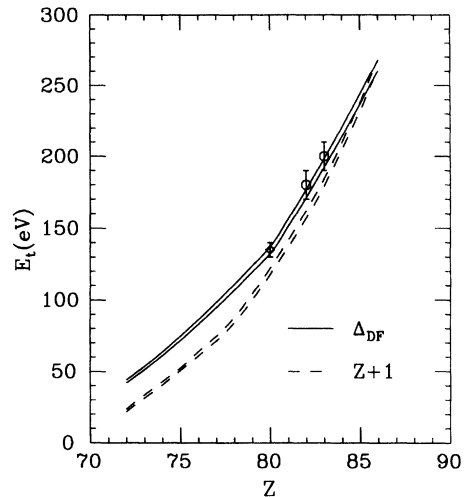


FIG. 5. Comparison of experimental values for $[2p4f]$ energy onsets and theoretical estimates as a function of the atomic number Z in sixth-period elements. Experimental values for the pure elements have been determined in this work (open circles) and in Ref. 11 (open diamond). Theoretical estimates (Ref. 11) calculated as differences of total-energy SCF-DF calculations for the configurations $E([2p_{3/2}4f_{7/2}]5f_{7/2}) - E([2p_{3/2}])$ (lower solid curve), and $E([2p_{3/2}4f_{5/2}]5f_{5/2}) - E([2p_{3/2}])$ (upper solid curve) are in nice agreement with experimental data. Calculated values obtained using the $Z + 1$ approximation (dashed curves) are also reported for comparison.

to possible strong-correlation effects in the $4f$ electronic shell.

Although the existence of these features is widely accepted as a general phenomenon, their contribution has been usually neglected in the interpretation of XAFS data of sixth-period atoms, in spite of the large number of studies performed at the edges under consideration. One possible reason is certainly associated with the presence of the structural signal, which can mask features due to the atomic background. Nevertheless, the presence of a nonmonotonic background can greatly affect the extraction of reliable structural parameters in the usual XAFS data analysis and therefore a correct modeling of the atomic background is certainly needed. Further studies of multielectron excitation contributions in XAFS spectra are highly desirable both for a better understanding of the atomic background and for improving the reliability of XAFS determination of local structure.

ACKNOWLEDGMENTS

We would like to thank the LURE staff, and in particular A. Sadoc and F. Villain, for technical assistance during the experiment. We gratefully thank F. Bizzarri (Università di Camerino) for his invaluable technical support. Part of this research has been financed through the TGE/CEE contract.

- ¹ S. J. Schaphorst, A. F. Kodre, J. Ruschinski, B. Crasemann, T. Åberg, J. Tulkki, M. H. Chen, Y. Azuma, and G. S. Brown, *Phys. Rev. A* **47**, 1953 (1993).
- ² A. Filipponi, T. A. Tyson, K. O. Hodgson, and S. Mobilio, *Phys. Rev. A* **48**, 1328 (1993).
- ³ A. Filipponi, E. Bernieri, and S. Mobilio, *Phys. Rev. B* **38**, 3298 (1988).
- ⁴ A. Di Cicco, S. Stizza, A. Filipponi, F. Boscherini, and S. Mobilio, *J. Phys. B* **25**, 2309 (1992).
- ⁵ A. Filipponi, S. Di Nardo, L. Lozzi, S. Santucci, and P. Picozzi, *Phys. Rev. B* **48**, 13 430 (1993).
- ⁶ A. Di Cicco, M. De Crescenzi, R. Bernardini, and G. Mancini, *Phys. Rev. B* **49**, 2226 (1994).
- ⁷ P. D'Angelo, A. Di Cicco, A. Filipponi, and N. V. Pavel, *Phys. Rev. A* **47**, 2055 (1993).
- ⁸ E. Burattini, P. D'Angelo, A. Di Cicco, A. Filipponi, and N. V. Pavel, *J. Phys. Chem.* **97**, 5486 (1993).
- ⁹ M. Deutsch and M. Hart, *Phys. Rev. A* **34**, 5168 (1986); E. Bernieri and E. Burattini, *ibid.* **35**, 3322 (1987); Y. Ito, H. Nakamatsu, T. Mukoyama, K. Omote, S. Yoshikado, M. Takahashi, and M. Emura, *ibid.* **46**, 6083 (1992).
- ¹⁰ G. Li, F. Bridges, and G. S. Brown, *Phys. Rev. Lett.* **68**, 1609 (1992).
- ¹¹ A. Filipponi, L. Ottaviano, and T. A. Tyson, *Phys. Rev. A* **48**, 2098 (1993).
- ¹² E. A. Stern, B. A. Bunker, and S. M. Heald, *Phys. Rev. B* **21**, 5521 (1980).
- ¹³ E. A. Stern and Ke Zhang, *Phys. Rev. Lett.* **60**, 1872 (1988).
- ¹⁴ J. B. Boyce, F. G. Bridges, T. Claeson, T. H. Geballe, G. G. Li, and A. W. Sleight, *Phys. Rev. B* **44**, 6961 (1991).
- ¹⁵ E. Sevillano, H. Meuth, and J. J. Rehr, *Phys. Rev. B* **20**, 4908 (1979).
- ¹⁶ A. Di Cicco (unpublished); A. Filipponi and A. Di Cicco, *Nucl. Instrum. Methods Phys. Res., Sect. B* (to be published).
- ¹⁷ L. Ottaviano, A. Filipponi, A. Di Cicco, P. Picozzi, and S. Santucci, *J. Non-Cryst. Solids* **156-158**, 112 (1993).
- ¹⁸ E. A. Stern, P. Līviņš, and Z. Zhang, *Phys. Rev. B* **43**, 8850 (1991).